Natural Resources for Human Health

eISSN: 2583-1194

Original Research

Received 27 July 2026
Revised 01 August 2026
Accepted 03 September 2026

Natural Resources for Human Health 2026, Vol. 6 (6): 262–276

KEYWORDS:
Pumpkin seed shell; activated carbon; phenol adsorption; biomass valorization; adsorption mechanism; wastewater treatment; biomass valorization.

Valorization of pumpkin seed shells into activated carbon for phenol adsorption: characterization, mechanisms, isotherms, and thermodynamics.

Mohammed Adel Mesbahi [1], Adel Khiouani [2,*], Salah Eddine Hachani [3,4], Oussama Khaoua [2], Sofiane Makhloufi [5,6], Abdelhek Meklid [7], Ammar Zobeidi [8,9], Abdellatif Aouragh [2], Meriem Lebbal, Tahani-Achouak Chinar [2,10].

[1] Laboratory of Applied Chemistry and Environment. Faculty of Exact Sciences. University of El Oued. 39000 El Oued. Algeria.
[2] Laboratory of Materials Chemistry and the Livings: Activity and Reactivity (LCMVAR), Faculty of Matter Sciences, Department of Chemistry, University of Batna 1, Algeria.
[3] Faculty of Exact Sciences, Department of Chemistry, VTRS Laboratory, University of El Oued, El Oued, Algeria
[4] Department of Process Engineering & Petrochemistry, Faculty of Technology, University of El Oued, El Oued, 39000, Algeria.
[5] University of Biskra, Laboratory of Molecular Chemistry and Environment, 07000 Biskra Algeria.
[6] University of Djelfa, Faculty of technology, 17000, Djelfa Algeria.
[7] Laboratory of Applied Chemistry (LCA), University of Biskra, BP 145, 07000 Biskra, Algeria.
[8] Pollution & Waste Treatment Laboratory (PWTL). University of Ouargla. PO Box 511. Ouargla 30000. Algeria.
[9] Department of Chemistry. Faculty of Exact Sciences. University of El Oued. PO Box 789. El-Oued 39000. Algeria.
[10] Common Core Science and Technology Mustapha Ben Boulaid University Batna 2, Batna, 05000, Algeria.

ABSTRACT: The valorization of agricultural residues into functional adsorbents offers a sustainable approach for the removal of phenolic contaminants from water. In this study, activated carbon was prepared from pumpkin seed shells through carbonization and chemical activation and evaluated for phenol removal from aqueous solution. The physicochemical properties of the resulting carbon were investigated by scanning electron microscopy (SEM) and Brunauer–Emmett–Teller (BET) analysis, revealing a well-developed porous structure with a specific surface area of 629.84 $m^2 g^{-1}$, pore volume of 0.227 $cm^3 g^{-1}$, and average pore diameter of 54.26 Å. Batch adsorption experiments were performed to assess the effects of adsorbent dosage, contact time, and solution pH. Under the investigated conditions, an optimum adsorbent dosage of 0.20 g and pH close to 7 afforded an experimental adsorption capacity of 31.75 mg g^{-1}, with equilibrium approached after approximately 150 min. Among the tested kinetic models, the pseudo-second-order model provided the best fit (R^2 = 0.998), with a calculated equilibrium capacity of 34.01 mg g^{-1}. Equilibrium data were better described by the Freundlich model

Natural Resources for Human Health
eISSN: 2583-1194

(R^2 = 0.981) than by the Langmuir and Temkin models, indicating adsorption on a heterogeneous surface. Thermodynamic analysis yielded negative ΔG° values and a negative ΔH° (−3.50 kJ mol^{-1}), indicating a spontaneous and exothermic adsorption process. Overall, the results demonstrate the potential of pumpkin seed shell-derived activated carbon as a low-cost and sustainable adsorbent for phenol removal from aqueous media.

1. INTRODUCTION

Phenol is a priority organic contaminant frequently detected in industrial effluents, particularly those associated with petroleum refining, coal conversion, petrochemical processing, resin and plastic manufacturing, pharmaceutical production, and related chemical industries. Its high-water solubility, toxicity, and adverse effects on aquatic ecosystems and human health make the efficient treatment of phenol-containing wastewater an important environmental challenge [1–3]. Even at relatively low concentrations, phenolic compounds can impair water quality and pose risks to biological systems, highlighting the need for effective treatment technologies before industrial effluents are discharged into receiving waters [2,4]. A variety of physicochemical and biological technologies have been investigated for phenol removal, including membrane separation, advanced oxidation processes, biological degradation, solvent extraction, ion exchange, and thermal treatments [3–6]. However, the applicability of these technologies can be constrained by factors such as energy consumption, operational complexity, membrane fouling, generation of secondary pollutants, and treatment cost. Among the available approaches, adsorption has attracted sustained interest because of its operational simplicity, versatility, relatively low energy requirement, and potential for treating organic contaminants over a broad concentration range [4,7]. Recent reviews have confirmed adsorption as one of the most extensively investigated approaches for phenolic wastewater treatment, while also emphasizing that adsorption performance is strongly governed by the physicochemical properties of the adsorbent and operating conditions [4,8].

Activated carbon remains one of the most effective adsorbent classes for the removal of phenol and other aromatic organic contaminants because of its developed pore network, high specific surface area, and tunable surface chemistry [1,9]. The adsorption of phenolic compounds is influenced by several interrelated factors, including pore size distribution, surface functional groups, adsorbate characteristics, solution pH, ionic strength, temperature, initial pollutant concentration, and contact time [1,8,10]. Consequently, the development of activated carbons with suitable textural and surface properties is essential for achieving efficient phenol removal. Recent studies have particularly emphasized biomass-derived activated carbons as promising alternatives to conventional carbonaceous materials because they combine pollutant removal with renewable-resource utilization and waste valorization [11,12]. The production of activated carbon from lignocellulosic residues generally involves carbonization followed by physical or chemical activation. Carbonization promotes the formation of a carbon-rich framework through the removal of volatile components, whereas activation develops porosity and modifies the surface chemistry, thereby generating adsorption sites with enhanced accessibility [9,11]. Physical activation commonly employs oxidizing gases such as CO2 or steam at elevated temperatures, whereas chemical activation uses activating agents to promote pore development and can provide substantial textural modification at comparatively lower temperatures [11–13]. The nature of the precursor and activation route therefore plays a decisive role in determining the pore structure, surface area, surface functionality, and ultimately the adsorption performance of the resulting carbon material.

Agricultural residues represent particularly attractive precursors because their abundance, renewable character, low economic value, and carbon-rich composition can support the preparation of value-added adsorbents while contributing to waste minimization [11–13]. A wide range of biomass residues, including nutshells, fruit stones, agricultural stalks, husks, shells, and other lignocellulosic wastes, has been explored for the preparation of activated carbons for water treatment [11,12]. Recent investigations have demonstrated that biomass-derived activated carbons can exhibit substantial adsorption performance toward phenolic contaminants, while adsorption behavior remains highly dependent on activation conditions and the resulting surface characteristics [12,14]. Despite the extensive literature on biomass-derived activated carbons, the valorization of pumpkin seed shells as a precursor for phenol-removing activated carbon remains comparatively underexplored. Pumpkin seed processing generates substantial quantities of shell residues that are commonly treated as low-value agricultural waste. Converting this residue into a porous adsorbent could therefore provide a dual environmental benefit by reducing biomass

waste while producing a material for wastewater remediation. Moreover, establishing the relationship between adsorption performance and operational parameters is necessary for evaluating the practical potential of such a material [15,18].

Accordingly, the present study investigates the preparation of activated carbon from pumpkin seed shells through carbonization and chemical activation and evaluates its potential for phenol removal from aqueous solution. The resulting material was characterized in terms of surface morphology and textural properties using scanning electron microscopy (SEM) and Brunauer–Emmett–Teller (BET) analysis. The effects of adsorbent dosage, contact time, and solution pH on phenol adsorption were systematically investigated. In addition, adsorption kinetics were evaluated using pseudo-first-order, pseudo-second-order, and intraparticle-diffusion models, while equilibrium behavior was assessed using Langmuir, Freundlich, and Temkin isotherms. Finally, thermodynamic parameters were determined to clarify the spontaneity and thermal nature of the adsorption process. This integrated approach provides insight into the adsorption behavior of phenol on pumpkin seed shell-derived activated carbon and assesses its potential as a sustainable biomass-based adsorbent for aqueous-phase phenol remediation.

2. EXPERIMENTAL METHODS

2.1. Preparation of activated carbon

Pumpkin seed shells were collected, thoroughly washed with distilled water to remove adhering impurities, and dried at 107 °C for 24 h. The dried shells were subsequently subjected to thermal treatment at 310 °C for 50 min using a heating rate of 7 °C min^{-1}. The resulting carbonized material was ground and mixed with an aqueous NaOH solution using a carbonized-material-to-NaOH mass ratio of 2:1. The mixture was allowed to stand for 24 h to promote impregnation of the activating agent. The impregnated precursor was then thermally activated at 590 °C for 1 h. After activation, the material was treated with 1.0 M HCl to remove residual inorganic species and soluble reaction products, followed by repeated washing with distilled water until the washing solution was free of residual acid. The resulting activated carbon was dried at 107 °C for 24 h and stored in a sealed glass container until further use.

2.2. Characterization

The morphology and surface structure of the prepared activated carbon were examined by scanning electron microscopy (SEM) using a VEGA 3 TESCAN microscope operated at an accelerating voltage of 20 kV. The textural properties of the activated carbon were determined by nitrogen adsorption–desorption measurements using a Mercer instrument. The specific surface area was calculated according to the Brunauer–Emmett–Teller (BET) method. The resulting surface area and pore characteristics were used to assess the development of the porous structure following carbonization and chemical activation.

2.3. Phenol adsorption experiments

Batch adsorption experiments were conducted to evaluate the performance of the pumpkin seed shell-derived activated carbon toward phenol removal from aqueous solution. The effects of adsorbent dosage, contact time, and solution pH were investigated over the experimental ranges of 50–350 mg of adsorbent, 0–300 min, and pH 4–11, respectively. Unless otherwise specified, 200 mg of activated carbon was contacted with 100 mL of phenol solution in polyethylene tubes. The suspensions were agitated at 150 rpm in a thermostatically controlled water bath. At predetermined contact times, the activated carbon was separated from the suspension, and the residual phenol concentration was determined by UV–visible spectrophotometry. For the spectrophotometric analysis, 1 mL of the phenol-containing solution was transferred to a clean colorimetric tube and diluted with deionized water to a final volume of 50 mL. A 0.5 mL aliquot of buffer solution was then added to maintain the required analytical conditions. The absorbance was measured at 270 nm using an EVOLUTION 220 UV–visible spectrophotometer. The equilibrium adsorption capacity, qe (mg $g^{-}1$), and phenol removal efficiency, RERE (%), were calculated using Eqs. (1) and (2), respectively [19]:

$$RE(\%) = \frac{C_0 - C_e}{C_0} \times 100 \quad (1)$$

$$q_e = \frac{V}{W}(C_0 - C_e) \quad (2)$$

where C_0 and Ce are the initial and equilibrium phenol concentrations (mg L^{-1}), respectively, V is the volume of the phenol solution (L), and mm is the mass of activated carbon (g).

2.3.1. Adsorption kinetic models

To elucidate the adsorption kinetics and identify the possible rate-controlling steps during phenol uptake, the experimental kinetic data were analyzed using pseudo-first-order (PFO), pseudo-second-order (PSO), and intraparticle diffusion models. The PFO and PSO models were used to evaluate the kinetic behavior of phenol adsorption, whereas the intraparticle diffusion model was applied to assess the contribution of diffusion within the porous structure to the overall adsorption process (19). Comparison of the corresponding kinetic parameters and goodness-of-fit values provides complementary information on the adsorption rate and the mechanisms potentially governing phenol transport and uptake.

2.3.2. Adsorption equilibrium models

The equilibrium adsorption behavior of phenol was evaluated using the Langmuir, Freundlich, and Temkin isotherm models. The Langmuir model describes adsorption on a relatively homogeneous surface with a finite number of energetically equivalent sites, whereas the Freundlich model accounts for adsorption on a heterogeneous surface with a distribution of adsorption energies. The Temkin model additionally considers changes in adsorption energy associated with adsorbate–adsorbent interactions as the surface coverage increases (19). Comparison of these models was therefore used to assess the equilibrium characteristics and adsorption capacity of the prepared activated carbon.

2.3.3. Adsorption thermodynamics

The thermodynamic characteristics of phenol adsorption were investigated using equilibrium data obtained at different temperatures. The standard Gibbs free energy change ($\Delta G°$), standard enthalpy change ($\Delta H°$), and standard entropy change ($\Delta S°$) were determined to evaluate the spontaneity, energetic nature, and entropy changes associated with the adsorption process (19). These parameters provide a thermodynamic framework for interpreting the interaction between phenol molecules and the surface of the prepared activated carbon.

3. RESULTS AND DISCUSSION

3.1 SEM results

The surface morphology of an activated carbon is closely related to its adsorption performance because surface texture and pore development influence the accessibility of adsorption sites. Figure 1 presents SEM micrographs of the prepared activated carbon at different magnifications. The images reveal a heterogeneous and relatively rough surface characterized by irregular morphological features and visible cavities. Such surface characteristics are consistent with the development of a porous structure during the activation process and may favor the accessibility of phenol molecules to the adsorbent surface [20,21]. However, SEM observations provide primarily morphological information and should therefore be considered together with quantitative textural characterization. The N_2 adsorption–desorption analysis presented below provides complementary information on the specific surface area and pore characteristics of the material.

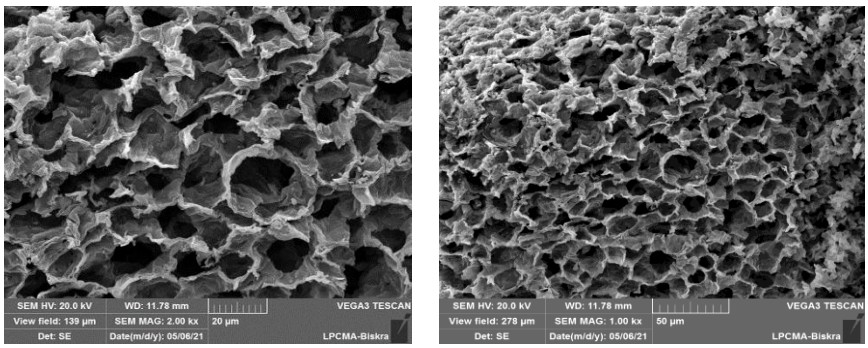


Figure 1. SEM images of the prepared activated carbon at different magnifications.

3.2. BET results

The textural properties of the prepared activated carbon were investigated by N_2 adsorption–desorption analysis. The specific surface area, pore volume, and pore diameter are important parameters for evaluating the development and accessibility of the porous structure and, consequently, the potential availability of adsorption sites (22). As shown in Figure 2, the prepared activated carbon exhibited a specific surface area of 629.8374 m^2/g, a pore volume of 0.226960 cm^3/g, and an average pore

diameter of 54.257 Å (5.426 nm). The relatively high specific surface area indicates the development of an accessible porous surface during activation. Moreover, the average pore diameter of approximately 5.43 nm falls within the mesoporous range according to the conventional IUPAC classification. The coexistence of substantial surface area and mesopores may facilitate the transport of phenol molecules toward accessible adsorption sites. Nevertheless, adsorption performance is governed not only by surface area but also by pore accessibility and the physicochemical interactions between phenol and the carbon surface.

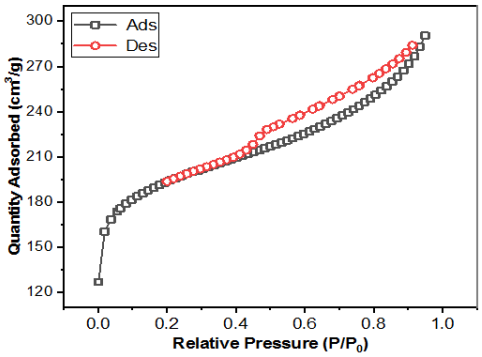


Figure 2. N_2 adsorption–desorption isotherm of the prepared activated carbon.

3.3. Adsorption results

3.3.1. Effect of adsorbent mass

The effect of activated-carbon dosage on phenol adsorption was investigated by varying the adsorbent mass, and the corresponding results are presented in Figures 3 (a, b) . Increasing the adsorbent dosage resulted in an increase in phenol removal efficiency. This behavior is expected because increasing the mass of activated carbon increases the total number of available adsorption sites and the overall surface area accessible to phenol molecules. As the adsorbent dosage increases, a larger fraction of the phenol initially present in solution can therefore be removed. At higher adsorbent dosages, however, the increase in removal efficiency becomes progressively less pronounced. This tendency indicates that the adsorption system approaches a condition in which the amount of available phenol becomes insufficient to proportionally utilize the additional adsorption sites provided by the increased adsorbent mass. In contrast to the removal efficiency, the equilibrium adsorption capacity (q_e), expressed per unit mass of adsorbent, decreased as the activated-carbon dosage increased. This apparent inverse relationship is commonly observed in batch adsorption systems and can result from the distribution of a relatively fixed amount of phenol among an increasing number of adsorption sites. At higher solid concentrations, particle aggregation may also reduce the effective surface area accessible to the adsorbate, potentially contributing to the decrease in q_e. Considering both the removal efficiency and adsorption capacity, an activated-carbon dosage of 0.2 g was selected for the subsequent experiments. Under these conditions, an equilibrium adsorption capacity of 31.75 mg/g was obtained. This dosage was therefore considered an appropriate compromise between the amount of adsorbent used and the resulting phenol uptake.

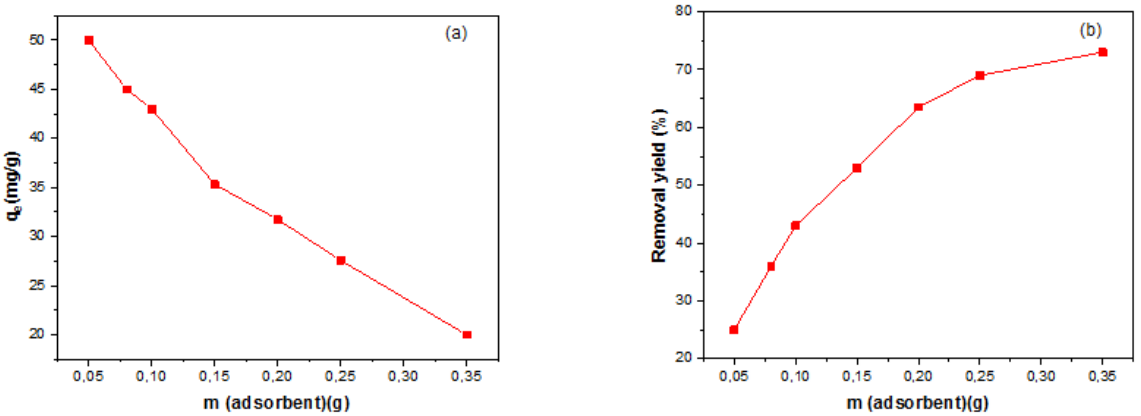


Figure 3. (a) Variation in adsorption capacity and (b) phenol removal efficiency as a function of activated-carbon dosage.

3.3.2. Effect of contact time on adsorption

The influence of contact time on phenol adsorption is presented in Figure 4. The adsorption capacity increased progressively with increasing contact time, indicating rapid initial phenol uptake followed by a slower approach toward equilibrium. After approximately 150 min, the adsorption capacity reached 31.5 mg/g, indicating that the system had approached equilibrium under the investigated conditions. A slight additional increase was observed after 24 h, giving a final adsorption capacity of 31.75 mg/g. The relatively rapid adsorption observed during the initial stage can be attributed to the high availability of unoccupied adsorption sites and the concentration gradient between the aqueous phase and the activated-carbon surface. As adsorption proceeds, these sites become progressively occupied and the concentration gradient decreases, leading to a reduction in the adsorption rate. The subsequent small increase in q_e indicates that adsorption continued after 150 min, although at a considerably lower rate, until a practically stable adsorption capacity was reached. The contact-time profile therefore indicates a two-stage adsorption behavior consisting of a relatively rapid initial uptake followed by a slower approach toward equilibrium. The equilibrium time determined from these experiments was subsequently used as the basis for the adsorption studies performed under the selected experimental conditions.

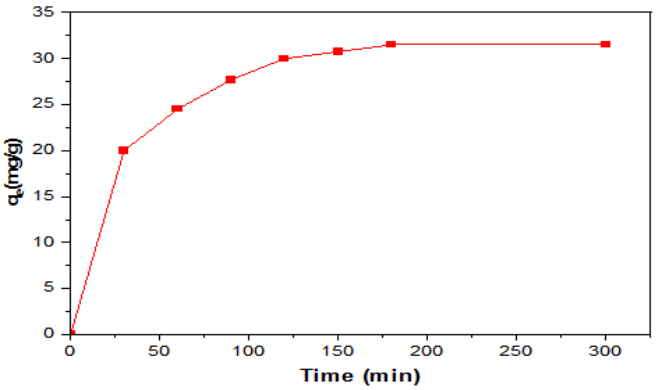


Figure 4. Variation in adsorption capacity as a function of contact time.

3.3.3. Effect of pH on adsorption

Solution pH is a critical parameter in phenol adsorption because it can simultaneously influence the ionization state of the adsorbate and the surface-charge characteristics of the activated carbon. Changes in these properties can consequently modify the interactions between phenol species and the adsorbent surface [19]. The effect of pH was investigated over the range 5.2–10.1, as shown in Figure 5. The highest adsorption/removal performance was observed at pH 7.2. The observed dependence cannot be attributed simply to the equality of H_3O^+ and OH^- concentrations, since such equality corresponds to neutral pH under specific temperature and solution conditions and does not, by itself, determine the adsorption behavior. The observed optimum at pH 7.2 is more appropriately interpreted in terms of the combined effects of phenol speciation and the surface-charge characteristics of the activated carbon. Phenol has a pK_a of approximately 10, meaning that it remains predominantly in its neutral molecular form throughout most of the investigated pH range, although increasing deprotonation becomes increasingly relevant as the pH approaches the pK_a. Consequently, the adsorption behavior in the investigated range may be governed by a combination of surface–phenol interactions, hydrogen bonding, π-related interactions, and electrostatic contributions associated with changes in surface charge. The maximum adsorption observed at pH 7.2 therefore identifies this condition as the most favorable among those investigated. This pH was subsequently selected for the adsorption experiments to provide a consistent basis for evaluating the effects of the other experimental parameters.

The adsorption behavior was strongly influenced by solution pH. The activated carbon surface contains functional groups that can undergo protonation and deprotonation depending on the solution pH, thereby modifying its surface charge and its interactions with phenol molecules. At lower pH values, the increased concentration of H_3O^+ can protonate negatively charged surface functionalities, altering the surface charge and the balance of adsorbent–adsorbate interactions. As the pH increases, progressive deprotonation of surface groups can modify the electrostatic environment at the adsorbent–solution interface and

consequently affect phenol uptake. The maximum adsorption performance was observed at pH 7.2. This behavior is likely associated with the combined effects of the surface charge of the activated carbon, phenol speciation, and the physicochemical interactions established at the solid–liquid interface. Because the pKa of phenol is approximately 10, phenol remains predominantly in its neutral molecular form throughout most of the investigated pH range, while increasing deprotonation becomes increasingly important as the pH approaches 10. Therefore, the decrease in adsorption at higher pH values may reflect changes in surface–adsorbate interactions rather than simply the presence of OH^- ions. Accordingly, pH 7.2 was selected as the optimum condition for subsequent adsorption experiments.

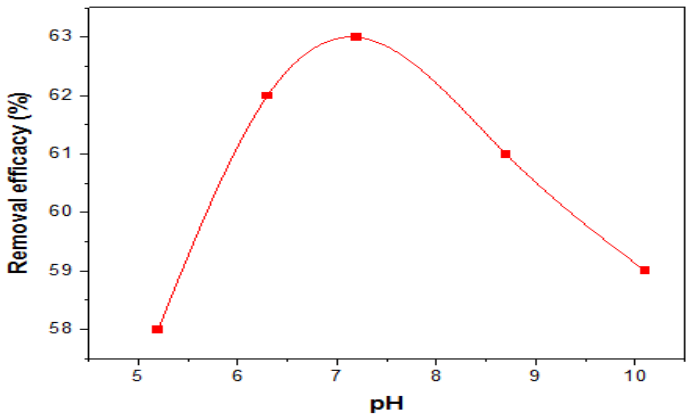


Figure 5. Effect of solution pH on phenol adsorption onto the prepared activated carbon.

3.4. Adsorption isotherm models

Adsorption isotherm analysis was performed to elucidate the equilibrium behavior of phenol on the prepared activated carbon. Three classical models, Langmuir, Freundlich, and Temkin, were applied to the experimental equilibrium data. These models provide complementary information regarding the surface characteristics, adsorption heterogeneity, and energetic interactions involved in phenol uptake.

3.4.1. Langmuir isotherm model

The Langmuir model assumes that adsorption occurs on a finite number of energetically equivalent sites and that each site can accommodate one adsorbate molecule. The model is based on monolayer adsorption, with no lateral interactions between adsorbed molecules and no variation in adsorption energy among the available sites. The Langmuir equation used in this study is expressed as follows [23]:

$$\frac{C_e}{q_e} = \frac{1}{q_{max} K_L} + \frac{1}{q_{max}} C_e \qquad (5)$$

where: K_L is the Langmuir constant (L.mg^{-1}), and q_{max} is the maximum monolayer adsorption capacity (mg.g^{-1}). The corresponding Langmuir plot is presented in Figure 6.

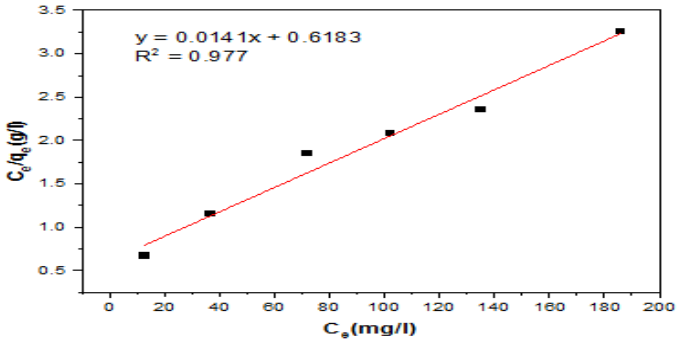


Figure 6. Langmuir isotherm plot for phenol adsorption onto the prepared activated carbon.

Natural Resources for Human Health
eISSN: 2583-1194

3.4.2. Freundlich isotherm model

The Freundlich model is an empirical isotherm that describes adsorption on energetically heterogeneous surfaces characterized by a distribution of adsorption affinities. Unlike the Langmuir model, it does not assume a uniform population of adsorption sites or a single adsorption energy. The Freundlich equation used in this study is given by [24].:

$$lnq_e = lnk_F + \frac{lnC_e}{n} \qquad (4)$$

Where: K_F is the Freundlich constant (mg.g^{-1}.mg$^{-1/n}$.L$^{-1/n}$), and n is the Freundlich constant related to adsorption intensity .The corresponding Freundlich plot is presented in Figure 7.

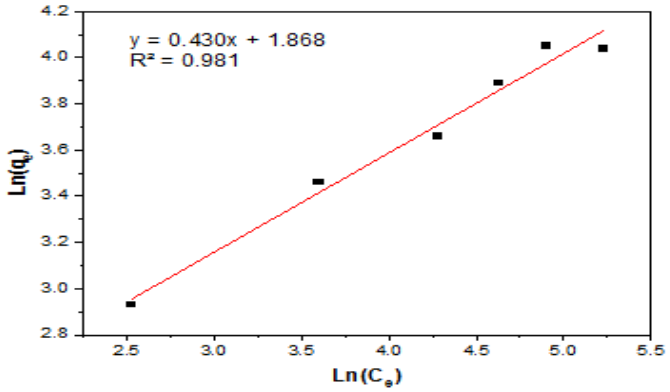


Figure 7. Freundlich isotherm plot for phenol adsorption onto the prepared activated carbon.

3.4.3. Temkin isotherm model

The Temkin model considers adsorbent–adsorbate interactions and assumes that the heat of adsorption decreases approximately linearly with increasing surface coverage as a consequence of interactions between adsorbed species. The model therefore provides information about the energetic characteristics of adsorption over the investigated concentration range. The Temkin equation used in this study is expressed as follows [25]:

$$q_e = \left(\frac{RT}{b_T}\right) lnK_T + \left(\frac{RT}{b_T}\right) ln\ C_e \qquad (5)$$

where: K_T is the Temkin constant (L.g^{-1}), b_T is the equilibrium binding constant (J.mol^{-1}), R is the ideal gas constant (8.314 J.mol^{-1}.K^{-1}), and T is the absolute temperature (K). The corresponding Temkin plot is presented in Figure 8.

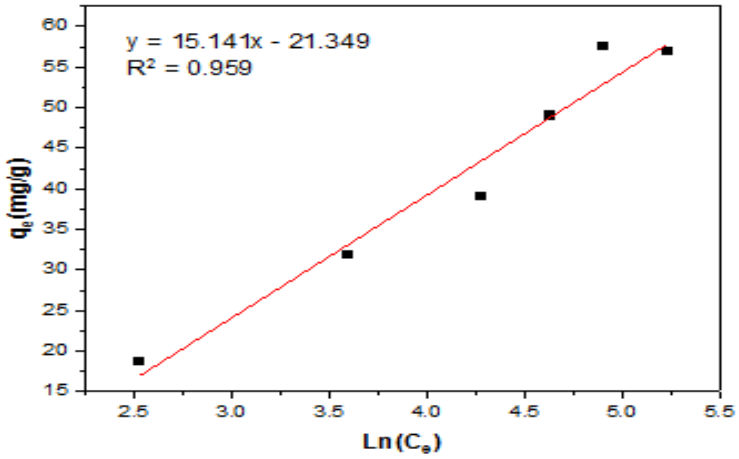


Figure 8. Temkin isotherm plot for phenol adsorption onto the prepared activated carbon.

The experimental equilibrium data were fitted to the Langmuir, Freundlich, and Temkin models, and the corresponding parameters are summarized in Table 1. Among the three models, the Freundlich model provided the best fit to the experimental data, with an R^2 value of 0.981. The higher correlation obtained for the Freundlich model compared with the Langmuir and Temkin models indicates that the equilibrium adsorption behavior is better described by a heterogeneous surface model than by the assumptions of a homogeneous Langmuir surface.

The good agreement with the Freundlich model suggests that the prepared activated carbon possesses adsorption sites with different affinities toward phenol, which is consistent with the heterogeneous nature expected for carbonaceous materials containing different surface functionalities and pore environments. However, the superior Freundlich fit should not be interpreted as definitive evidence of multilayer adsorption, since the Freundlich equation is an empirical model and its parameters do not uniquely establish the number of adsorption layers. Rather, the results indicate that surface heterogeneity and a distribution of adsorption energies play an important role in the equilibrium adsorption of phenol (Table 1). Thus, the isotherm analysis indicates that phenol adsorption onto the prepared activated carbon is more appropriately described by heterogeneous adsorption behavior than by an idealized homogeneous monolayer model.

Table 1. Different adsorption isotherms.

Langmuir isotherm model			Freundlich isotherm model			Temkin isotherm model		
K_L (L/mg)	q_{max} (mg/g)	R^2	K_F (mg/g)	n	R^2	K_T	b_t ((kJ/mol)	R^2
0.0228	70.9220	0.977	6.4760	2.3261	0.981	0.2441	0.1636	0.959

3.5. Adsorption kinetics

The adsorption kinetics of phenol onto the prepared activated carbon were investigated using the pseudo-first-order (PFO), pseudo-second-order (PSO), and intraparticle diffusion models. The corresponding model parameters are presented in Table 2, while the fitted kinetic plots are shown in Figures 10–12. Comparison of the correlation coefficients and calculated equilibrium adsorption capacities was used to determine which kinetic model best represented the experimental adsorption data.

3.5.1. Pseudo-first-order kinetic model

The pseudo-first-order model, originally proposed by Lagergren, assumes that the adsorption rate is proportional to the difference between the equilibrium adsorption capacity and the amount of adsorbate adsorbed at a given time. The corresponding equation used to describe the experimental data is given by [26]:

$$\ln(q_e - q_t) = lnq_e - K_1 \qquad (6)$$

where q_e and q_t are the adsorption capacities at equilibrium and at time t, respectively, and k_1 is the pseudo-first-order rate constant. The corresponding linearized PFO plot is presented in Figure 9.

Natural Resources for Human Health
eISSN: 2583-1194

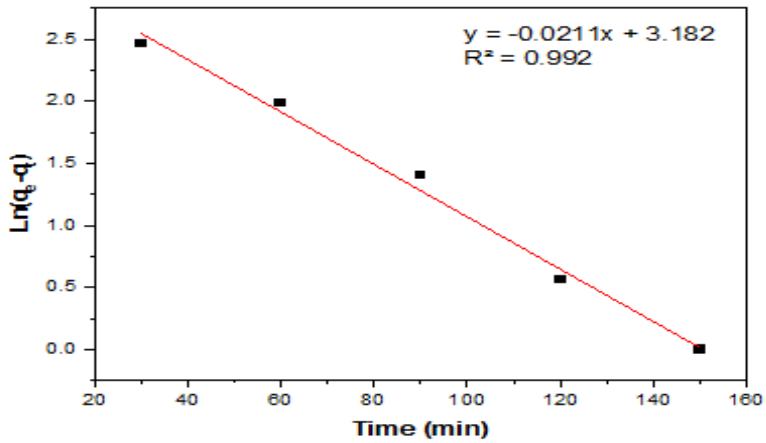


Figure 9. Pseudo-first-order kinetic plot for phenol adsorption onto the prepared activated carbon.

3.5.2. Pseudo-second-order kinetic model

The pseudo-second-order model describes the adsorption rate as being proportional to the square of the difference between the equilibrium adsorption capacity and the adsorption capacity at a given time. The equation applied to the experimental data is given by [27,28]:

$$\frac{t}{q_t} = \frac{1}{q_e^2 K_2} + \frac{t}{q_e} \qquad (7)$$

where k_2 is the pseudo-second-order rate constant. The corresponding PSO plot is shown in Figure 10.

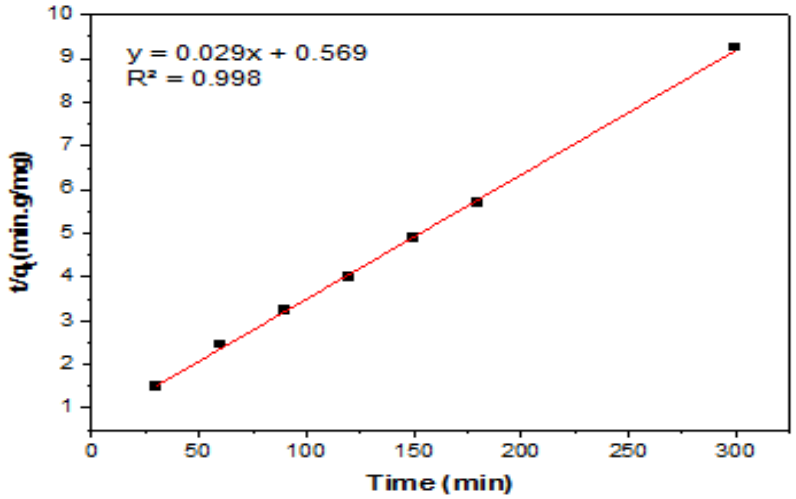


Figure 10. Pseudo-second-order kinetic plot for phenol adsorption onto the prepared activated carbon.

It should be noted that a better fit to the pseudo-second-order model does not, by itself, establish that adsorption proceeds through covalent bonding or a specific chemisorption mechanism. The PSO model is a kinetic model, and its parameters should therefore be interpreted primarily in terms of the rate behavior of the adsorption system. Evidence for chemisorption should instead be based on complementary characterization or mechanistic analyses.

Natural Resources for Human Health
eISSN: 2583-1194

3.5.3. Intraparticle diffusion model

The intraparticle diffusion model was applied to evaluate whether diffusion within the porous structure of the activated carbon contributes to the overall adsorption rate. The model is expressed as follows [29]:

$$q_t = k_{int} t^{0.5} + C \quad (8)$$

where q_t is the adsorption capacity at time t, k_{int} is the intraparticle diffusion rate constant, and C is the intercept associated with the boundary-layer effect. The corresponding plot is presented in Figure 11.

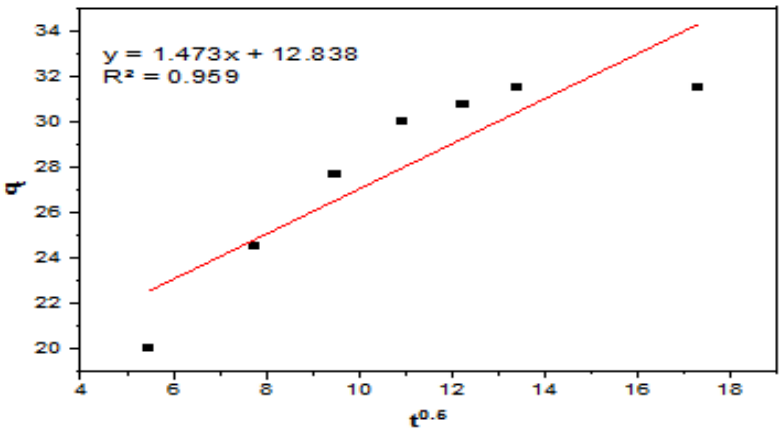


Figure 11. Intraparticle diffusion plot for phenol adsorption onto the prepared activated carbon.

The kinetic parameters obtained from the three models are summarized in Table 2. The pseudo-second-order model provided the highest correlation coefficient (R^2 = 0.998), compared with R^2 = 0.991 for the pseudo-first-order model and R^2 = 0.959 for the intraparticle diffusion model. In addition, the equilibrium adsorption capacity calculated from the PSO model (q_e,cal = 34.0136 mg/g) was reasonably close to the experimental value (q_e,exp = 31.75 mg/g). These results indicate that the pseudo-second-order equation provides the best mathematical description of the experimental kinetic data among the models considered. However, the difference between q_e,cal and q_e,exp should also be acknowledged rather than describing the agreement as exact. The intraparticle diffusion model exhibited a lower correlation coefficient (R^2 = 0.959), indicating that intraparticle diffusion alone does not adequately describe the overall adsorption kinetics.

Table 2. Kinetic parameters for phenol adsorption onto the prepared activated carbon.

Model	Parameter	Value
PFO	q_e,exp (mg/g)	31.75
	q_e,cal (mg/g)	24.0949
	k_1 (min^{-1})	0.0211
	R^2	0.991
PSO	q_e,exp (mg/g)	31.75
	q_e,cal (mg/g)	34.0136
	k_2 (g mg^{-1} min^{-1})	0.0015
	R^2	0.998
Intraparticle diffusion	k_{int} (mg g^{-1} min^{-1})	1.4733
	C (mg/g)	12.8380
	R^2	0.959

Furthermore, the non-zero intercept obtained from the intraparticle diffusion model (C = 12.8380 mg/g) suggests that intraparticle diffusion is not the sole rate-controlling step and that boundary-layer effects or other mass-transfer processes may

also contribute to phenol uptake. Thus, the adsorption kinetics are better described as a combination of surface and diffusion-related processes rather than by a single transport mechanism.

3.6. Thermodynamic functions results

The thermodynamic characteristics of phenol adsorption onto the prepared activated carbon were evaluated using the equilibrium data obtained at different temperatures. The selected experimental conditions included an adsorbent mass of 0.2 g, an initial phenol concentration of 100 mg/L, a solution volume of 100 mL, and a contact time of 24 h. Under these conditions, an equilibrium adsorption capacity of 31.75 mg/g was obtained. The standard Gibbs free energy change (ΔG°), standard enthalpy change (ΔH°), and standard entropy change (ΔS°) were determined to assess the spontaneity and energetic characteristics of the adsorption process. The corresponding equations are given in Eqs. (9 –12) [19]:

$$\ln k_d = \frac{\Delta S^\circ}{R} - \frac{\Delta H^\circ}{RT} \quad (9)$$

$$k_d = \frac{q_e}{C_e} \quad (10)$$

$$\Delta G^\circ = -RT \ln k_d \quad (11)$$

The values of ΔH° and ΔS° were determined from the slope and intercept, respectively, of the van't Hoff plot (ln K_d vs. 1/T), as presented in Figure 12.

As shown in Table 3, the negative values of ΔG° indicate that phenol adsorption onto the prepared activated carbon is thermodynamically favorable under the investigated temperature conditions. The magnitude and temperature dependence of ΔG° provide an indication of the driving force of the adsorption process. The negative value of ΔH° indicates that the adsorption process is exothermic, meaning that heat is released during phenol uptake. Consequently, increasing the temperature is expected to be unfavorable to adsorption if the equilibrium data exhibit the corresponding decrease in adsorption capacity. The exothermic character is consistent with the formation of favorable interactions between phenol molecules and the activated-carbon surface. The sign and magnitude of ΔS° should be interpreted according to the experimentally determined value. A negative ΔS° would indicate a decrease in the overall configurational freedom of the system upon adsorption, consistent with the transfer of phenol molecules from the aqueous phase to relatively constrained adsorption sites on the carbon surface. Conversely, a positive ΔS° would indicate an increase in the overall disorder associated with the adsorption process, potentially resulting from changes in the hydration or interfacial structure accompanying adsorption. Thus, the thermodynamic parameters provide complementary evidence that phenol adsorption is thermodynamically favorable and exothermic under the investigated conditions, while the entropy contribution provides additional information about changes occurring at the adsorbent–solution interface

.

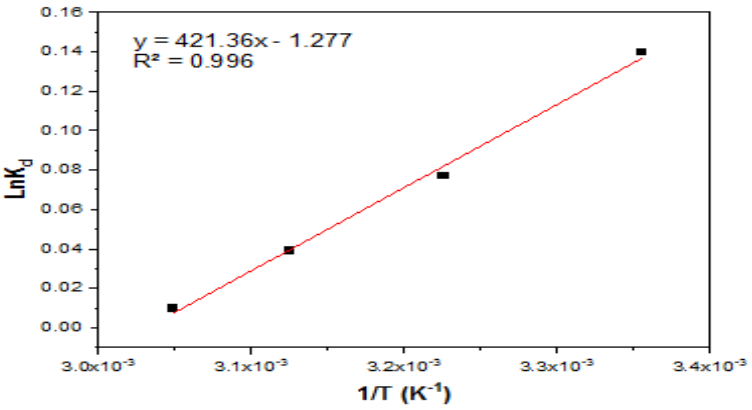


Figure 12. The variations of Lnk_d as a function of 1/T.

Table 3. Thermodynamic parameter of the studied adsorption process.

T (K)	K_d	ΔG° (kJ/mol)	ΔH° (kJ/mol)	ΔS° (J/mol K)
298	1.15	-0.346360	- 3.5032	- 10.619
310	1.08	-0.198500		
320	1.04	-0.104290		
328	1.01	-0.269970		

4. Conclusion

This study demonstrates the potential of activated carbon derived from pumpkin seed shells as a sustainable adsorbent for phenol removal from aqueous media. The activation treatment produced a highly porous carbon with a BET surface area of 629.84 $m^2\ g^{-1}$ and a pore volume of 0.227 $cm^3\ g^{-1}$, providing favorable characteristics for adsorption. The adsorption performance was strongly dependent on the operating conditions, with an optimum adsorbent dosage of 0.20 g and a solution pH close to 7. An experimental adsorption capacity of 31.75 mg g^{-1} was achieved, with equilibrium approached after approximately 150 min. The adsorption kinetics were best represented by the pseudo-second-order model ($R^2 = 0.998$), whose calculated equilibrium capacity (34.01 mg g^{-1}) was consistent with the experimental value. Equilibrium analysis showed that the Freundlich model provided the best correlation ($R^2 = 0.981$), suggesting that phenol adsorption occurs on a heterogeneous adsorbent surface. The thermodynamic results further indicated a spontaneous and exothermic process, as reflected by the negative $\Delta G°$ values and $\Delta H°$ of −3.50 kJ mol^{-1}. Overall, the findings highlight the feasibility of converting pumpkin seed shell waste into a value-added porous carbon material for phenol removal. The combination of agricultural-waste valorization, favorable textural properties, and effective adsorption performance supports its potential application in sustainable wastewater treatment. Further studies under continuous-flow conditions and with real industrial wastewater would be valuable to assess its practical applicability and regeneration performance.

ACKNOWLEDGEMENTS

The authors gratefully acknowledge the support of the DGRSDT (Algerian Ministry of Higher Education and Scientific Research, MESRS).

AUTHOR CONTRIBUTIONS

Mohammed Adel M. Writing – review & editing, Writing – original draft, Methodology, Laboratory Analysis.
Adel K, Meriem L. Writing – original draft, Visualization, Methodology, Investigation, Formal analysis, Data curation.
Salah Eddine H. Writing – review & editing, Writing – original draft, Visualization, Validation, Resources,
Oussama K. Writing – review & editing, Writing – original draft, Supervision, Project administration, Methodology.
Sofiane M. Visualization, Validation, Supervision, Resources, Project administration, Methodology, Investigation, Funding acquisition, Formal analysis.
Abdelhek M. Resources, Data Curation, Formal Analysis.
Ammar Z Writing – review & editing, Writing – original draft, Visualization, Validation, Supervision, Resources, Project administration, Methodology.
Abdellatif A. Methodology, Investigation, Data curation.
Tahani-Achouak C. Validation, Supervision, Methodology, Conceptualization.

CONFLICT OF INTEREST

The authors declare that there is no conflict of interest.

ETHICS STATEMENT

This article does not contain any studies involving human participants or animals performed by any of the authors.

DATA AVAILABILITY STATEMENT

The data supporting the findings of this study are available from the corresponding author upon reasonable request.

REFERENCES

[1] Chand Meena, M.; Band, R.; Sharma, G. Phenol and its toxicity: a case report. IJT. 2015, 8,1222-1224. http://ijt.arakmu.ac.ir/article-1-383-en.html
[2] Gami, A.A.; Shukor, M.; Khalil, K.A.; Dahalan, F.A.; Khalid, A.; Ahmad, S.A. Phenol and its toxicity. Journal of Environmental Microbiology and Toxicology. 2014, 2, 11-23. https://doi.org/10.54987/jemat.v2i1.89

[3] Tišler, T.; Zagorc-Končan, J. Comparative assessment of toxicity of phenol, formaldehyde, and industrial wastewater to aquatic organisms. Water. Air. Soil. Pollut. 1997, 97, 315-322. https://doi.org/10.1023/A:1026472313561
[4] Breton, R.L.; Teed, R.S.; Moore D.R.J. An ecological risk assessment of phenol in the aquatic environment. HERA. 2003, 9, 549-568. https://doi.org/10.1080/713609922
[5] Otitoju, O.B.; Alfred, M.O.; Ogunlaja, O.O.; Olorunnisola, C.G.; Olukanni O.D.; Ogunlaja, A.; Omorogie, O.M.; Unuabonah, E.I. Pollution and risk assessment of phenolic compounds in drinking water sources from south-western Nigeria. Environ. Sci. Pollut. Res. 2023, 30, 76798-76817. https://doi.org/10.1007/s11356-023-27622-w
[6] Ahmaruzzaman, M.; Soumya, R.M.; Vishal, G.; Yadav, G.; Roy, S.; Bhattacharjee, B.; Bhuyan, A.; Hazarika, B.; Darabdhara, J.; Kumari, K. Phenolic compounds in water: from toxicity and source to sustainable solutions-an integrated review of removal methods, advanced technologies, cost analysis, and future prospects. J. Environ. Chem. Eng. 2024, 12, 112964. https://doi.org/10.1016/j.jece.2024.112964
[7] Ramos, R.L.; Victor, R.M.; Miriam, C.S.A.Phenolic compounds in water: review of occurrence, risk, and retention by membrane technology. JEM. 2024, 351, 119772. https://doi.org/10.1016/j.jenvman.2023.119772
[8] Sanchez-Arevalo, C.M.; Aldegheri, F.; Vincent-Vela, M.C.; Álvarez-Blanco, S. Integrated membrane process in organic media: combining organic solvent ultrafiltration, nanofiltration, and reverse osmosis to purify and concentrate the phenolic compounds from wet olive pomace. Int. J. Mol. Sci. 2024, 25, 5233. https://doi.org/10.3390/ijms25105233
[9] Benoumena, H., Zobeidi, A., Atia, S., Lakhdari, W., Dehliz, A., Bouhenna, M. M., & Mimouni, M. (2026). Comparative Performance of Commercial Versus Biosynthesized Chitosan Epichlorohydrin/Kaolinite Biocomposites for Methyl Orange Removal: Box Behnken Optimization, Adsorption Mechanism, and Density Functional Theory Calculations. International Journal of Aquatic Research and Environmental Studies, 6(2), 1131–1148. https://doi.org/10.70102/xs89sk25.
[10] Tesfaye, G.M.; Tessema, A.B.; Arumugasamy, S.K. (2025) In: Natural Resources-Based Activated Carbon Synthesis Encyclopedia of Green Materials. Springer, Singapore. https://doi.org/10.1007/978-981-97-4618-7_275
[11] Zhang, J.; Duan, C.; Huang, X.; Mianwu, M.; Li, Y.; Huang, H.; Wang, H.; Yan, M.; Tang, X. A review on research progress and prospects of agricultural waste-based activated carbon: preparation, application, and source of raw materials. J. Mater. Sci. 2024, 59, 5271-5292. https://doi.org/10.1007/s10853-024-09526-3
[12] Ferdous, A.R.; Shah, S.S.; Shaikh, M.N.; Barai, H.R.; Marwat, M.A.; Oyama, M.; Abdul Aziz, M. Advancements in biomass-derived activated carbon for sustainable hydrogen storage: a comprehensive review. Chem. Asian. J. 2024, 16, e202300780. https://doi.org/10.1002/asia.202300780
[13] Bazgir, H.; Rostami, M.R.; Tavakkol, S.; Issaabadi, Z.; Shirazi, H.M.; Goshayeshi, B.; M. Van Geem, K.; Haghighi, M.N.; Abbas-Abadi, M.S. The chemical process of producing activated carbon using walnut shells and plastic wastes. J. Therm. Anal. Calorim. 2023, 148, 10125-10138. https://doi.org/10.1007/s10973-023-12364-1
[14] Rashid, R.; Shafiq, I.; Akhter, P.; Iqbal, M.J.; Hussain, M. A state-of-the-art review on wastewater treatment techniques: the effectiveness of adsorption method. Environ. Sci. Pollut. Res. 2021, 28, 9050-9066. https://doi.org/10.1007/s11356-021-12395-x
[15] Babaami, N., Zobeidi, A., Zenkheri, L., Boudjema, S., Ben Azia, G., & Benhania, A. (2023). Wastewater treatment by improving the local clay capacity with chemical and thermal activation. Asian Journal of Water, Environment and Pollution, 20(6), 53–59. https://doi.org/10.3233/ajw230079.
[16] Hamidi, A., Atia, D., Rebiai, A., Reghioua, A., Zobeidi, A., Messaoudi, M., Seghir, B. B., Pohl, P., & Simal-Gandara, J. (2023). Investigation of adsorption kinetics and isothermal thermodynamics for optimizing methylene blue adsorption onto a modified clay with cellulose using the response surface approach. Biomass Conversion and Biorefinery. https://doi.org/10.1007/s13399-023-04397-1.
[17] Zhang, R.; Zeng, L.; Wang, F.; Li, X.; Li, Z. Influence of pore volume and surface area on benzene adsorption capacity of activated carbons in indoor environments. Build. Environ. 2022, 216, 109011. https://doi.org/10.1016/j.buildenv.2022.109011
[18] Bal, G.; Thakur, A. Distinct approaches of removal of dyes from wastewater: A review. Mater. Today. 2022, 50, 1575-1579. https://doi.org/10.1016/j.matpr.2021.09.119
[19] Khiouani, A.; Hachani, SE.; Meklid, A. Removal of Phenol from Water Using an Activated Carbon Prepared from Juniperus Thurifera Tree. Chem. Chem. Technol. 2023, 17, 636-645. https://doi.org/10.23939/chcht17.03.636
[20] Bahemmi, S., Zobeidi, A., Atia, S., Neghmouche Nacer, S., Ghernaout, D., and Elboughdiri, N. Activating illite kaolinite clay with CTAB for adsorbing methylene blue: isotherms, kinetics, and thermodynamics studies Tuijin Jishu/Journal of Propulsion Technology, Band. 2023, 44, 812-?. https://doi.org/10.52783/tjpt.v44.i5.2678

[22] El Nemr, A.; Abdelwahab, O.; El-Sikaily, O.; Khaled, A. Removal of direct blue-86 from aqueous solution by new activated carbon developed from orange peel. J. Hazard. Mater. 2009, 161, 102-110. https://doi.org/10.1016/j.jhazmat.2008.03.060
[22] Ma, Y.; Gao, N.; Chu, W.; Li, C. Removal of phenol by powdered activated carbon adsorption. Environ. Sci. Eng. 2013, 7, 158-165. https://doi.org/10.1007/s11783-012-0479-7
[23] Langmuir, I. The adsorption of gases on plane surfaces of glass, mica and platinum. J. Am. Chem. Soc. 1918, 40, 1361-1403. https://doi.org/10.1021/ja02242a004
[24] Freundlich, H.M.F. Over the adsorption in solution. J. Phys. Chem. 1906, 57, 385-471.
[25] Temkin, M.; Pyzhev, V. Kinetics of ammonia synthesis on promoted iron catalysts. Acta. physiochim. URSS. 1940, 12, 327-356.
[26] Lagergren, S. About the theory of so-called adsorption of soluble substancesKungliga Svenska Vetenskapsakademiens, Handlingar, Band. 1898, 24, 1-39.
[27] Ho, Y.S.; Mckay, G. Pseudo-second order model for sorption processes. Process. Biochem. 1999, 34, 451-465. https://doi.org/10.1016/S0032-9592(98)00112-5
[28] Mabrouk, S., Bebba, A. A., Kamarchou, A., and Zobeidi, A. Adsorption capacity of pollutants by using local clay mineral from urban wastewater Touggourt (South-East Algeria) Asian Journal of Research in Chemistry, Band. 2020, 13, 85-90. https://doi.org/10.5958/0974-4150.2020.00017.5.
[29] Atia, D., Bebba, A. A., Haddad, L., and Zobeidi, A. Elimination of organic pollutants from urban wastewater by illite-kaolinite local clay from south-east of Algeria Cienc. Tecn. Vitivinic, Band. 2018, 33, 17.